Characterization of phase singularities in the vector complex Ginzburg-Landau equation

Miguel Hoyuelos and Adrián Jacobo
Departamento de Física, Facultad de Ciencias Exactas y Naturales, Universidad Nacional de Mar del Plata, Funes 3350, 7600 Mar del Plata, Argentina

(Received 25 June 2004; revised manuscript received 13 October 2004; published 21 January 2005)

The vector complex Ginzburg-Landau equation is an amplitude equation appropriate for describing instabilities in oscillatory media when the order parameter is a vector field (for example, laser light or two-component Bose condensate). It is known that this equation presents a variety of phase singularities or topological defects. We study the parameters that characterize the different kinds of defects and show that the results are useful for a better understanding of the system dynamics.

DOI: 10.1103/PhysRevE.71.017203 PACS number(s): 05.45.−a, 42.65.Sf

I. INTRODUCTION

Spatially extended nonlinear dynamical systems present a great variety of behaviors including pattern formation, self-organization, and spatiotemporal chaos [1]. Many of them also display states with localized objects with some kind of particlelike behavior [2]. Complex patterns of nonlinear systems can sometimes be understood in terms of these particlelike objects.

Nonlinear optical cavities provide many examples of patterns with localized structures. They appear in the plane transverse to light propagation and can take the form of defects, vortices, or solitons (bright or dark). They have been observed or predicted in lasers [3], photorefractive materials [4], lasers or driven optical cavities with saturable absorbers [5], semiconductors [6], optical bistability [7], and second-order nonlinear optical oscillators [8]. Usually, the mathematical description of these optical systems is done in terms of a scalar field, since the polarization degree of freedom is considered to be fixed either by material anisotropies or by experimental arrangement. However, if the polarization of the light is not fixed, the vector nature of the electromagnetic field leads to new and interesting phenomena [9].

The complex Ginzburg-Landau (CGL) equation is the generic amplitude equation model that describes slow modulations in the oscillations of spatially coupled oscillators close to a Hopf bifurcation [1,10]. The vector complex Ginzburg-Landau (VCGL) equation has been derived in a variety of contexts, e.g., in the interaction of counterpropagating waves [11] or when the order parameter is of vectorial character, such as the electric field in large aperture lasers [12,13]. In the appropriate range of parameters, the VCGL equation also describes a two-component Bose condensate [14].

Different kinds of defects [15–20] are present in the two-dimensional (2D) VCGL equation. In this paper we consider quantities, such as size, frequency, or wave number of the wave emitted by the defect core, which characterize the different kinds of defects. We study the behavior of these quantities as functions of the parameters of the equation.

II. THE EQUATION

The VCGL equation can be written as

$$\frac{\partial A_\pm}{\partial t} = (1+i\alpha)\nabla^2 A_\pm - (1+i\beta)(|A_\pm|^2 + \gamma|A_\mp|^2 - 1)A_\pm. \tag{1}$$

[The scaling $A_\pm \to A_\pm \exp(-i\beta t)$ was used with respect to another version used in, e.g., Refs. [15–20], in order to have a nonoscillating homogeneous solution.] In the context of lasers, $A_\pm$ represent the circularly polarized right and left components, α represents the strength of diffraction, β is related to the frequency detuning, γ is the coupling parameter related to decay constants, and ∇^2 is the 2D transverse Laplacian. The definition of the equation parameters in terms of physical quantities can be found in Ref. [13].

The coupling parameter γ should satisfy the condition $\gamma > -1$ for the system to converge to a finite solution. We will consider that the condition $1+\alpha\beta > 0$ (Benjamin-Feir stability criterion) is satisfied, which means that there are always some plane waves that are stable against long wavelength perturbations. The family of plane wave solutions has the form, $A_\pm = Q_\pm e^{-i(\mathbf{k}_\pm \cdot \mathbf{r} - \omega_\pm t + \phi_{0\pm})}$. If $\gamma > 1$, the stable plane wave solution is circularly polarized. If $-1 < \gamma < 1$, the stable plane wave solution is, in general, elliptically polarized, and, if $k_+ = k_- = k$, we have a linearly polarized solution [20].

Starting from random initial conditions, even if the condition $1+\alpha\beta > 0$ is satisfied, the system usually does not evolve to a plane wave due to the presence of phase singularities or defects: points where the phase of the complex field, A_+ or A_- (or both), is not defined and the amplitude is zero. A spiral wave develops around each defect that, far from the defect core, approaches a plane wave.

Defects can be classified in two groups: vector and scalar defects. Vector defects are points where the two components, A_+ and A_-, vanish. Scalar defects are points at which only one of the two fields, A_+ or A_-, vanish. The following ansatz is used to describe the field around a defect in a stationary state, in polar coordinates with the origin at the defect core,

$$A_\pm(r,\theta) = R_\pm(r) e^{i n_\pm \theta + i\psi_\pm(r) + i\omega_\pm t}. \tag{2}$$

where $n_\pm$ is the topological charge of the singularity that necessarily takes integer values. Only defects with charges $n = \pm 1$ have been found in the scalar or vector Ginzburg-Landau equation. Defects with larger values of $|n|$ are un-

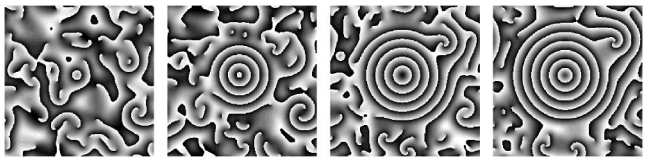

FIG. 1. Sum of the phases of A_+ and A_-. From left to right, the sequence corresponds to times 100, 700, 1300, and 1900. The initial condition is random. The global phase of the vector defect, which is approximately in the center, appears as a target pattern that grows with time. Parameters: $\alpha=0$, $\beta=1.29$, $\gamma=0.1$.

stable and detach in defects with smaller charge. (Defects with $|n|=2$ have been reported for the vector Swift-Hohenberg equation [21].) If $\gamma>1$, vector defects are not topologically allowed, since the stable homogeneous states are such that one of the two field components vanishes in large areas, not just at points.

In Eq. (2), $\omega_\pm$ is the rotation frequency of the spiral wave. For $r\to\infty$, $\psi_\pm(r)=k_\pm r$, where the spiral wave number $k_\pm$ far from the defect core is the one that corresponds to a plane wave and is given by $k_\pm^2=\omega_\pm/(\beta-\alpha)$.

The amplitudes of A_+ and A_- close to the core of a vector defect are written as $R_\pm(r)=(R_{\pm\infty}/r_0)r$, where $R_{\pm\infty}=\lim_{r\to\infty}R_\pm(r)$. The same relation holds for one of the components of a scalar defect. The linear relation between amplitude and distance r, when $r\simeq 0$, holds when the topological charge is ± 1 [22]. We consider the quantity r_0 as a measure of the defect size.

In summary, the parameters that characterize a defect are the charge $n_\pm$, size r_0 and frequency $\omega_\pm$ (or asymptotic wave number $k_\pm$).

One of the reasons to study in detail the defects of the VCGL equation is that this kind of localized structure often organizes the geometry and dynamics of the host medium, so that they become "building blocks" of regular patterns and of spatiotemporal chaos [2,23]. Figure 1 represents numerical integration [24] of Eq. (1) and shows an example where the whole system dynamics is governed by one defect.

It is clear that a detailed study of the defect parameters (r_0, $\omega_\pm$, or $k_\pm$) as functions of the parameters of Eq. (1) (α, β, and γ) would be useful for a better understanding of the dynamics. In order to simplify the analysis, we will restrict the study to the case $\alpha=0$, which, in an optical context, means that we are neglecting the effects of diffraction. This restriction can be done without loss of generality, at least when both components of the field have the same frequency, since the case $\alpha\neq 0$ can be recovered with an appropriate change of variables, which is a generalization to the vectorial case of the change of variables proposed in Ref. [22].

Taking $\alpha=0$, when we introduce the ansatz (2) in Eq. (1) we obtain the following real equations:

$$R_\pm''=-\frac{R_\pm'}{r}+\left(\psi_\pm'^2+\frac{n_\pm^2}{r^2}+R_\pm^2+\gamma R_\mp^2-1\right)R_\pm,$$

$$\psi_\pm''=-\frac{\psi_\pm'}{r}-\frac{2\psi_\pm'R_\pm'}{R_\pm}+\beta(k_\pm^2+R_\pm^2+\gamma R_\mp^2-1). \qquad (3)$$

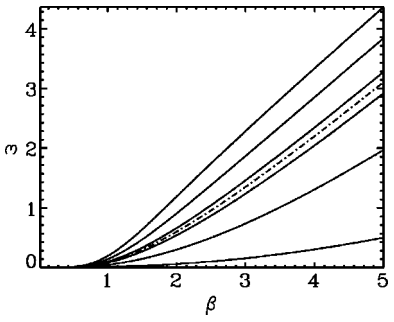

FIG. 2. Frequency ω_s of a symmetric scalar defect against β for different values of γ. From top to bottom, $\gamma=-0.9$, -0.5, -0.1, 0, 0.1, 0.5, and 0.9. The dashed line corresponds to the frequency ω_0 of a vector defect.

Numerical integration of Eq. (3) is a two point boundary problem that can be solved using a relaxation method [25]. In the next sections we present our results of the frequency and size of different kinds of defects as functions of parameters β and γ.

III. FREQUENCY AND COMPETITION AMONG DEFECTS

In Fig. 2, the dashed line shows the frequency as function of β for a vector defect; in an optical context, β represents the detuning, so, this result means that ω increases as the difference between atomic and cavity frequency increases.

The results for vector defects do not depend on neither γ (this parameter can be eliminated with a scaling of the amplitude [20]) nor the type of the vector defect (equal or opposite charges), and they are in agreement with the results of Hagan for a scalar defect [22]. Nevertheless, not every combination of parameters β and γ are allowed. Vector defects become unstable when γ approaches 1 [20]. Two mechanisms by which this process occurs have been identified: "domain instability" (the vector defect is annihilated by an external scalar defect) and "core instability" (the vector defect splits in two scalar defects). For small values of $|\gamma|$, there are theoretical limitations for the stability of vector defects. In Ref. [26] it is demonstrated, via a perturbative analysis for small $|\gamma|$, that two scalar defects in different components attract each other if $\beta>0.52$ and $\gamma>0$, or $\beta<0.52$ and $\gamma<0$.

For $-1<\gamma<1$, scalar defects can be symmetric or asymmetric. For a symmetric scalar defect, both components have the same amplitude far from the core, so, the background is linearly polarized. On the other hand, an asymmetric scalar defect has an elliptically polarized background; this is the case when scalar defects are in only one of the components of the field.

In Fig. 2, the frequency ω_s of a symmetric defect is plotted against β for different values of γ (the results for an asymmetric defect are qualitatively the same). In this plot, we can compare the frequency ω_s with the frequency ω_0 of a vector defect, which is the one that corresponds to $\gamma=0$. We can see that, if $\gamma>0$, then $\omega_0>\omega_s$, and, if $\gamma<0$, then $\omega_0<\omega_s$. It is known [27] that when a competition among wave emitting centers takes place, the oscillator with greater fre-

quency suppresses the waves produced by the others. Therefore, the previous results imply that if $\gamma>0$ the vector defect will dominate the dynamics at long times, while, if $\gamma<0$, the scalar defects will be dominant. Figure 1 shows a time sequence of a system with $\gamma=0.1$, starting from random initial conditions. A vector defect is spontaneously formed at the center of the system. The size of the defect domain grows with time, displacing the rest of the defects, which are most of them of scalar type. The vector defect imposes its frequency on the system. For $\gamma<0$, although isolated vector defects can be stable if $\beta<0.52$, starting from random initial conditions they cannot last because they cannot develop a domain as in Fig. 1, and they are not isolated from scalar defects that annihilate one of the components. This prediction was checked with numerical integration of Eq. (1).

IV. SIZE OF THE DEFECTS

The analysis of the size of the defects r_0 could be useful to compare it with the size of a real system in order to know if the defects are actually observable.

The size of a vector defect remains between 1.7 and 1.8 (see Ref. [13] to recover space units) for every value of parameter β. Much more important variations of r_0 appear for scalar defects as γ is varied.

In fact, r_0 of scalar defects diverges for $\gamma\to 1$ [16]. Let us consider γ close to 1, so that $\gamma=1-\delta\gamma$ with $|\delta\gamma|\ll 1$. We introduce a parameter ϵ, and change the space variable $r=x/\epsilon$, so that $R'_{\pm}\sim\epsilon$ and $R''_{\pm}\sim\epsilon^2$. Since the size of the defect is $r_0=R_{+\infty}/R'_{+}(0)$ (scalar defect in the "+" component), then $r_0\sim 1/\epsilon$. We can find a relation between ϵ and $\delta\gamma$ using Eq. (3), we get $1-R_{\mp}^2-R_{\pm}^2=O(\epsilon^2)/R_{\mp}-R_{\pm}^2\delta\gamma$. Combining both equations, we have $R_+R_-(R_++R_-)\delta\gamma=O(\epsilon^2)$. Since $R_+R_-(R_++R_-)=O(1)$, then $\epsilon\sim|\delta\gamma|^{1/2}$, and

$$r_0\sim\frac{1}{|1-\gamma|^{1/2}}. \tag{4}$$

For $\gamma>1$, linearly or elliptically polarized states become unstable with respect to circularly polarized states. Let us consider a scalar defect in the right, or "+," polarized phase with $n_+=\pm 1$ and $n_-=0$. As described in Ref. [16], for $\gamma>1$, it can be of two types: "repolarized core" defect or "punched core" defect. In the repolarized core structure, the "−" component takes nonzero values in the defect core region. On the other hand, in the punched core structure, the "−" component remains vanishing in the defect core region. Since the "−" component remains zero for the punched core structure, the defect is identical to those that appear in the scalar CGL equation. The size, frequency, or wave number of this defect does not depend on γ. Anyway, punched core defects are not allowed for every value of γ. Topological arguments discussed in Ref. [16] demonstrate that punched core defects cannot exist for γ slightly above 1. Numerically, we observe this kind of defects for $\gamma>1.5$. Therefore, when $\gamma>1$ Eq. (4) holds for repolarized core defects.

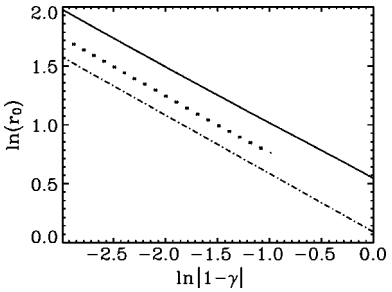

FIG. 3. Size r_0 against $|1-\gamma|$ in log-log scale for a symmetric scalar defect (continuous line, $\beta=0.1$) and for a repolarized core defect (dots, $\beta=1.29$). The dashed line has slope $-1/2$. This numerical result confirms Eq. (4).

Figure 3 shows the size r_0 of a symmetric scalar defect and for a repolarized core defect against $|1-\gamma|$ in log-log scale. The numerical results confirms the slope $-1/2$ of Eq. (4). There are not important variations of the size r_0 with parameter β.

V. CONCLUSIONS

We have numerically analyzed the different kinds of defects of the VCGL equation (1). We have considered the size of the defect core and frequency of the emitted spiral wave, as the quantities that characterize a defect. We have analyzed them as functions of the parameters of the VCGL equation: β and γ. The analysis is simplified by taking parameter $\alpha=0$. When both components of the field have the same frequency, the case $\alpha\neq 0$ can be recovered with a change of variables. For vector defects (for $-1<\gamma<1$) and punched core defect (for $\gamma>1$) the situation is even simpler since the properties of the defect do not depend on γ, and they depend only on β.

The size of scalar defects for $\gamma<1$ (symmetric and asymmetric defects) and for $\gamma>1$ (repolarized core defect) diverges as γ approaches 1. This theoretical result is numerically confirmed.

We have identified competition processes among defects where those with the greatest frequency imposes its wave over the system.

In summary, we have described the main characteristics of the defects in the VCGL equation via a thorough numerical study in the whole parameter space. In addition to the basic understanding of the dynamics in vector nonlinear media, the analysis of this kind of localized structure could be useful for information storage and processing.

ACKNOWLEDGMENTS

M.H. thanks M. San Miguel, E. Hernández-García, P. Colet, and G. Izús for helpful discussions. This work was partially supported by Consejo Nacional de Investigaciones Científicas y Técnicas (CONICET, Argentina, Grant No. PIP 4342/96) and Agencia Nacional de Promoción Científica y Tecnológica (ANPCyT, Argentina, Grant No. PICTO 2000-2001, No. 03-08431).

[1] M. C. Cross and P. C. Hohenberg, Rev. Mod. Phys. **65**, 851 (1993).
[2] H. Riecke, in *Pattern Formation in Continuous and Coupled Systems*, edited by M. Golubitsky, D. Luss, and S. H. Strogatz (Springer, New York, 1999); L. M. Pismen, *Vortices in Nonlinear Fields* (Oxford University Press, New York, 1999).
[3] D. Dangoisse, D. Hennequin, C. Lepers, E. Louvergneaux, and P. Glorieux, Phys. Rev. A **46**, 5955 (1992); N. R. Heckenberg *et al.*, Opt. Quantum Electron. **24**, S951 (1992).
[4] F. T. Arecchi *et al.*, Phys. Rev. Lett. **67**, 3749 (1991); K. Staliunas, G. Slekys, and C. O. Weiss, *ibid.* **79**, 2658 (1997); C. O. Weiss *et al.*, Appl. Phys. B: Lasers Opt. **B68**, 151 (1999).
[5] N. N. Rosanov, in *Progress in Optics*, edited by E. Wolf (North-Holland, Amsterdam, 1996), Vol. 35; W. Firth and A. J. Scroggie, Phys. Rev. Lett. **76**, 1623 (1996).
[6] M. Brambilla *et al.*, Phys. Rev. Lett. **79**, 2042 (1997); D. Michaelis, U. Peschel, and F. Lederer, Phys. Rev. A **56**, R3366 (1997).
[7] M. Tlidi, P. Mandel, and R. Lefever, Phys. Rev. Lett. **73**, 640 (1994).
[8] C. Etrich, U. Peschel, and F. Lederer, Phys. Rev. Lett. **79**, 2454 (1997); K. Staliunas and J. V. Sánchez-Morcillo, Phys. Rev. A **57**, 1454 (1998); G. L. Oppo, A. J. Scroggie, and W. J. Firth, J. Opt. B: Quantum Semiclassical Opt. **1**, 133 (1999).
[9] R. Bhandari, Phys. Rep. **281**, 1 (1997).
[10] W. van Saarloos, in *Spatio-Temporal Patterns in Non-Equilibrium Complex Systems*, edited by P. E. Cladis and P. Palffy-Muhoray (Addison-Wesley, Reading, MA, 1994).
[11] M. van Hecke, C. Storm, and W. van Saarloos, Physica D **134**, 1 (1999).
[12] M. San Miguel, Phys. Rev. Lett. **75**, 425 (1995).
[13] M. San Miguel, Q. Feng, J. V. Moloney, and A. C. Newell, in *Fluctuation Phenomena: Disorder and Nonlinearity*, edited by A. Bishop, S. Jimenez, and L. Vazquez (World Scientific, Singapore, 1995).
[14] R. Graham and D. Walls, Phys. Rev. A **57**, 484 (1998).
[15] L. Gil, Phys. Rev. Lett. **70**, 162 (1993).
[16] L. M. Pismen, Physica D **73**, 244 (1994); L. M. Pismen, Phys. Rev. Lett. **72**, 2557 (1994).
[17] E. Hernández-García, M. Hoyuelos, P. Colet, M. San Miguel, and R. Montagne, Int. J. Bifurcation Chaos Appl. Sci. Eng. **9**, 2257 (1999).
[18] M. Hoyuelos, E. Hernández-García, P. Colet, and M. San Miguel, Comput. Phys. Commun. **121–122**, 414 (1999).
[19] E. Hernández-García, M. Hoyuelos, P. Colet, and M. San Miguel, Phys. Rev. Lett. **85**, 744 (2000).
[20] M. Hoyuelos, E. Hernández-García, P. Colet, and M. San Miguel, Physica D **174**, 176 (2003).
[21] M. Hoyuelos and M. dell'Erba, Phys. Rev. E **68**, 065604(R) (2003).
[22] P. S. Hagan, SIAM (Soc. Ind. Appl. Math.) J. Appl. Math. **42**, 762 (1982).
[23] M. van Hecke, Phys. Rev. Lett. **80**, 1896 (1998).
[24] The integration method is seudospectral and second-order accurate in time. Lattices of size 128×128 were used. For more details, see Ref. [18].
[25] W. H. Press, S. A Teukolsky, W. T. Vetterling, and B. P. Flannery, *Numerical Recipes in Fortran 77* (Cambridge University Press, Cambridge, 1992).
[26] I. S. Aranson and L. M. Pismen, Phys. Rev. Lett. **84**, 634 (2000).
[27] A. S. Mikhailov, *Foundations of Synergetics I. Distributed Active Systems* (Springer, New York, 1990).